

## Surface Recombination Investigation in Thin 4H-SiC Layers

Karolis GULBINAS<sup>1\*</sup>, Vytautas GRIVICKAS<sup>1</sup>, Haniyeh P. MAHABADI<sup>2</sup>,  
Muhammad USMAN<sup>2</sup>, Anders HALLÉN<sup>2</sup>

<sup>1</sup> Institute of Applied Research, Vilnius University, Saulėtekio al. 10, LT-10222 Vilnius, Lithuania

<sup>2</sup> Royal Institute of Technology, KTH-ICT, P.O. Box Electrum 229, SE 164 40 Kista-Stockholm, Sweden

Received 18 November 2010; accepted 21 March 2011

n- and p-type 4H-SiC epilayers were grown on heavily doped SiC substrates. The thickness of the p-type layer was 7  $\mu\text{m}$  and the doping level around  $10^{17} \text{ cm}^{-3}$ , while the n-type epilayers were 15  $\mu\text{m}$  thick and had a doping concentration of  $3-5 \times 10^{15} \text{ cm}^{-3}$ . Several different surface treatments were then applied on the epilayers for surface passivation: SiO<sub>2</sub> growth, Al<sub>2</sub>O<sub>3</sub> deposited by atomic layer deposition, and Ar-ion implantation. Using collinear pump – probe technique the effective carrier lifetimes were measured from various places and statistical lifetime distributions were obtained. For surface recombination evaluation, two models are presented. One states that surface recombination velocity (SRV) is equal on both the passivation/epi layer interface ( $S_2$ ) and the deeper interface between the epilayer and the SiC substrate ( $S_1$ ), i. e. ( $S_1 = S_2$ ). The other model is simulated assuming that SRV in the epilayer/substrate ( $S_1$ ) interface is constant while in the passivation layer/epilayer ( $S_2$ ) interface SRV can be varied  $S_2 < S_1$ . Empirical nomograms are presented with various parameters sets to evaluate  $S_2$  values. We found that on the investigated 4H-SiC surfaces  $S_2$  ranges from  $3 \times 10^4$  to  $5 \times 10^4$  assuming that the bulk lifetime is 4  $\mu\text{s}$ . In Ar<sup>+</sup> implanted surfaces  $S_2$  is between ( $10^5 - 10^6$ ) cm/s.

*Keywords:* surface recombination velocity; carrier lifetime; silicon carbide.

### INTRODUCTION

Silicon carbide (SiC) is a promising semiconductor material for new or improved high-power, high frequency and high-temperature applications due to its outstanding properties such as high breakdown field, wide band gap and good thermal conductivity [1]. The chemical vapour deposition (CVD) method provides a solution to control the thickness of samples by homoepitaxial growth on commercial SiC wafers and to grow layers of regulated n-type or p-type doping level. However, considering the fact that surfaces and interfaces of thin epilayer are separated within a carriers diffusion length, surface recombination losses compared to those in the bulk may emerge as a prevalent device lifetime-limiting factor [2].

This work is oriented towards the effort to achieve a better surface passivation technique when using 4H-SiC epilayers for field transistor applications. We investigated four 4H-SiC epitaxial layers where the surfaces were treated in a different ways. Our aim was to evaluate the relative trend of surface recombination velocity (SRV) depending on the passivation scheme in order to find critical points for the quick evaluation of sample parameters. First, the effective excess carrier lifetimes in an epilayer was measured optically under moderate high-level injection. Afterwards a graphical solution with multiple nomograms describing the SRV were presented and compared with experimental results. We have developed a simple formula, which is valid for an intermediate case ( $S_2 < S_1$ ). Comparison of these formulas with the experimental data allows testing the ability of other technological recipes for passivation solutions and optimization in order to fulfill the requirements of both surface quality and high performance in the device.

### SAMPLES PREPARATION

4H-SiC epilayers were grown by hot-wall CVD on n-type 4H-SiC substrates obtained from “SiCrystal” AG company. The doping level of the substrate was of about  $1 \times 10^{19} \text{ cm}^{-3}$ . Both n- and p-type epilayers were grown. The n-type layer thickness was 15  $\mu\text{m}$  and the nitrogen doping level was about  $3-5 \times 10^{15} \text{ cm}^{-3}$ , while the p-type layer had a thickness of 7  $\mu\text{m}$  and an Al concentration of about  $10^{17} \text{ cm}^{-3}$  (only partly activated at room temperature). 1  $\text{cm}^2$  samples were cut from these wafers and the samples were then treated by three different techniques to accomplish various degrees of surface passivation. On one n-type sample a 50 nm SiO<sub>2</sub> film was grown at 1250 °C in N<sub>2</sub>O ambient. One n-type and one p-type sample was covered by 80 nm Al<sub>2</sub>O<sub>3</sub> deposited by thermal atomic layer deposition (ALD) at 250 °C, using the precursors – trimethyl aluminum (TMA) for Al and H<sub>2</sub>O for the oxide. The final sample, an n-type sample covered by a native oxide film was bombarded at room temperature with argon ions at an energy of 30 keV to produce a damaged layer just beneath the front surface of about 20 nm thickness.

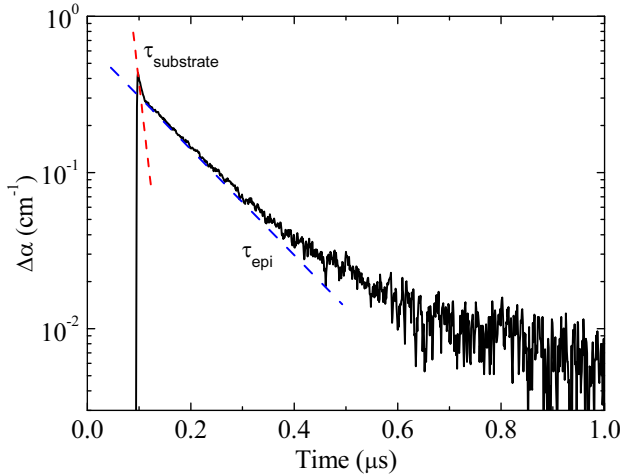
Moreover, on the same sample three different Ar doses were assembled by increasing implantation time into successive areas. One region was left unimplanted as a reference, resulting in a 1  $\text{cm}^2$  sample with four (2–3) mm wide stripes having implantation doses of  $3 \times 10^{13}$ ,  $3 \times 10^{14}$ , and  $3 \times 10^{15} \text{ cm}^{-2}$ , respectively. The highest two doses are expected to produce an amorphous layer, while the lowest dose will produce a defected, but still crystalline surface layer. It is also expected that a natural SiO<sub>2</sub> film will form, since the samples are exposed to air. No annealing was done on these samples prior to the measurements.

All samples were polished from the back side to provide good optical quality surfaces for the optical pump-

\*Corresponding author. Tel.: +370-5-2366079; fax: +370-5-2366059.  
E-mail address: karolis.gulbinas@ff.stud.vu.lt (K. Gulbinas)

**Table 1.** Summary of sample growth parameters

Sample type and oxide for passivation (SiC/oxide)	Total sample thickness ( $\mu\text{m}$ )	Epilayer thickness ( $\mu\text{m}$ )	Epilayer doping ( $\text{cm}^{-3}$ )	Oxide film	Film thick-ness (nm)
n-type (SiC/SiO <sub>2</sub> )	348 $\pm$ 2	15	(3–5) $\times 10^{15}$	SiO <sub>2</sub>	50
n-type SiC/Al <sub>2</sub> O <sub>3</sub>	350 $\pm$ 2	15	(3–5) $\times 10^{15}$	Al <sub>2</sub> O <sub>3</sub>	80
p-type SiC/Al <sub>2</sub> O <sub>3</sub>	340 $\pm$ 4	7	1 $\times 10^{17}$	Al <sub>2</sub> O <sub>3</sub>	80
n-type SiC/SiO <sub>2</sub> + Ar implanted	362 $\pm$ 2	15	(3–5) $\times 10^{15}$	Native Oxide	2 (Ar damage depth 20 nm)

**Fig. 1.** Experimental carrier transient with characteristic lifetime values shown for sample with surface passivated by SiO<sub>2</sub> film: exponential lifetime in the substrate and the effective lifetime in the epilayer is indicated by dashed lines

probe measurements. A summary of the sample parameters is given in Table 1.

## MEASUREMENT TECHNIQUE

To measure carrier lifetime transients collinear pump-probe technique was used [3]. Pump pulses with linear polarization are generated by a Q-switched Infinity Nd:YAG laser tripled to output of 355 nm (3.49 eV). Filters were used to keep constant energy per pulse which, was 13  $\mu\text{J}$ . The laser pulse half-width was 2 ns and the repetition rate was 40 Hz. The pump beam excited the surface at approximately 30° degrees angle to the epilayer plane and the spot size was approximately 0.5 mm<sup>2</sup>. Generated electron-hole pairs were probed with a 40 mW infrared 861 nm wavelength continuous laser beam. The probe beam was focused to a spot of  $\sim 10 \mu\text{m}$  in diameter, which penetrated the sample perpendicularly to the layer plane and then was guided with lenses into a fast photo receiver (response time – 0.5 ns). Carrier transients were observed on a 2 GHz oscilloscope screen and recorded by a computer. Raw signal data were recalculated into induced absorption coefficients and effective carrier lifetime was extracted from the slope of the induced absorption decay [3].

Each sample was attached to a holder on a movable table which was controlled using step motors with micrometer precision. This setup allowed performing measurements in different spots on the same sample. Every new measuring position was shifted at least 100  $\mu\text{m}$  away from former one. For each sample 20–40 different positions were measured.

## RESULTS

Excess carrier transient after laser pulse excitation is shown in Fig. 1. Similar ones are measured in other samples. The absorption coefficient decay comprises of three characteristic parts which can be distinguished: a fast one, an intermediate decay and a slow tail. The fast component accounts for lifetime shorter than 15 ns. It is assigned to carrier recombination in the substrate where a substantial fraction of excess carrier density is generated because the laser light penetration depth is  $\sim 50 \mu\text{m}$  [4]. Fast component depends primarily on the ratio of substrate lifetimes to the duration of laser pulse. In a FCA experiments, fast component amplitude varies on the polarization and wavelength of the probe light [5]. For 861 nm wavelength and  $E \perp C$  polarization used in the current work, the fast component amplitude is smaller than for corresponding 1300 nm probe wavelength utilized in our previous experiments for 2 ns pulse duration pulses [2, 3]. The intermediate component refers to effective carrier lifetime [6] in the epilayer,  $\tau_{\text{epi}}$ , which is of the main importance in the current investigation. The remaining tail of the decay is caused by carrier trapping in the substrate since, after time elapsing, separation of excess electrons and holes builds up due to remaining carrier leakage over the epilayer/substrate interface [7]. While the sum of the three recombination processes gives a resultant experimental curve like in Fig. 1, a natural subtraction of the slow component with slow apparent decay time (and a fast one with a single exponent) may involve substantial mistake in  $\tau_{\text{epi}}$  determination. The slow component is expected to be of very small amplitude within time span of 1–2  $\tau_{\text{epi}}$ . Thus, slow decay has no significant importance to our measurements and will not be analyzed further. We applied most simple way to extract  $\tau_{\text{epi}}$  by fitting an exponential slope for the initial part of the intermediate decay (see Fig. 1). Over four investigated samples in total two hundred transient have been analyzed and corresponding  $\tau_{\text{epi}}$  values were determined.

Our measurements are performed under ambipolar level injection condition ( $\Delta n = \Delta p \gg n_0, p_0$ ):

$$\Delta n = \Delta p = \frac{(1-R) \cdot E \cdot \alpha}{h\nu \cdot 1.602 \cdot 10^{-19} \cdot S}, \quad (1)$$

where  $\Delta n = \Delta p$  corresponds to the averaged excess carrier density in the epilayer;  $n_0, p_0$  – equilibrium concentration of electrons (in n-type) and holes (in p-type);  $R$  – reflectivity (0.25);  $E$  – the pulse energy of 13  $\mu\text{J}$ , which was assumed constant for all measurements;  $\alpha$  – the absorption coefficient for 355 nm is about  $\sim 200 \text{ cm}^{-1}$ ;  $h\nu$  – the quantum energy of 355 nm light (3.49 eV);  $S$  – spot

area, which was about  $0.5 \text{ mm}^2$ . For given values we calculated that injection of excess carrier density in the epilayer was  $\sim 7 \times 10^{17} \text{ cm}^3$ . The recombination lifetime under these conditions is the same value for both holes and electrons. No Auger recombination occurs in 4H-SiC under these injection conditions [7].

Extracted effective carrier lifetimes  $\tau_{\text{epi}}$  for each sample is shown in Fig. 2 where average value and standard spread in the sample are shown. The longest lifetimes are observed in 4H-SiC n-type samples with  $\text{SiO}_2$  and  $\text{Al}_2\text{O}_3$  oxides which vary around 120 ns. The lowest lifetime is observed in a sample with p-type  $\text{Al}_2\text{O}_3$  oxide and it is about 40 ns. The sample bombarded with argon indicates carrier lifetimes of 58 ns–70 ns. No significant difference in the regions with different doses of argon was observed. Moreover, the reference region with no implantation exposure indicates a mean carrier lifetime of 71 ns. This suggests that Ar-ion implantation slightly reduced the effective lifetime in the epilayer, but there is no dose dependence.

The dashed line in Fig. 2 represents the carrier lifetime in the substrate extracted from the fast transient during the first 10 ns–20 ns of the decay. All samples indicated a fast component which was faster than 15 ns (Fig. 1). Because we cannot distinguish location of recombination processes from the carrier transient the carrier lifetime in the substrate is a lower constrain of our measurement. Neither shorter nor equal to substrate carrier lifetimes can be distinguished.

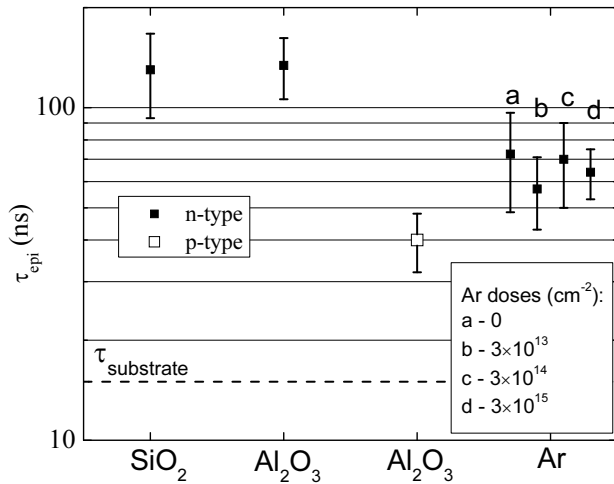


**Fig. 2.** Extracted effective lifetime  $\tau_{\text{eff}}$  in the epilayers with different surface treatment:  $\text{SiO}_2$  and  $\text{Al}_2\text{O}_3$  oxides and bombarded with argon ions. Regions with different doses of Ar implantation are indicated with letters. Error bar shows the standard spread

Long carrier lifetime is obtained for bulk 4H samples where recombination is described only by inner processes and no lifetime reduction occurs from surface recombination. Bulk lifetime  $\tau_{\text{bulk}}$ , thus, is the upper boundary of our simulation. In 4H-SiC  $\tau_{\text{bulk}}$  varies depending on quality and growth technique. Since we do not know the precise  $\tau_{\text{bulk}}$  value for this particular case we are going to assume a top value of 4  $\mu\text{s}$  for all 4H-SiC samples in order to exaggerate the input from the surface recombination.

## EVALUATION MODEL

As a first step towards the proper combination of the recombination processes involved, we present a direct model that involves analytical solutions of the fundamental mode of the excess carrier lifetime in a thin epitaxial slab by using the simple one-dimensional equation [8]:

$$\frac{\Delta n(x,t)}{\partial t} = D \frac{\partial^2 \Delta n(x,t)}{\Delta x^2} - \frac{\Delta n(x,t)}{\tau_b} \quad (2)$$

with two boundary conditions:  $S = S_2$ ,  $x = 0$  and  $S = S_1$ ,  $x = d$ :

$$\Delta n(t)|_{x=0,d} = \frac{D}{S} \cdot \frac{\Delta n(x,t)}{\partial x}, \quad (3)$$

where  $S$  is the surface recombination velocity defined in the usual manner [9] and the generation function is of the form:

$$\Delta n(x,t) = \Delta n_0 \exp(-\alpha x) \delta(t). \quad (4)$$

Here notations used:  $d$  is thickness of the epilayer and  $D$  is excess carrier diffusion coefficient,  $\delta(t)$  is the unit impulse function of generated carriers. The average carrier density in the epilayer can be defined as:

$$\Delta n(t) = \frac{1}{d} \int_0^d \Delta n(x,t) dx \quad (5)$$

and the instantaneous lifetime is defined as:

$$\tau^{-1} = -\frac{d}{dt} \ln \Delta n(t). \quad (6)$$

Due to a sufficiently high value of the carrier mobility and corresponding ambipolar diffusivity  $D \approx 3.5 \text{ cm}^2/\text{s}$  in 4H-SiC, the ratio  $Sd/D \leq 1$  is fulfilled for the  $\sim 10 \mu\text{m}$  thick epitaxial slabs for practical recombination velocities  $S_1, S_2 > 10^3 \text{ cm/s}$ . In this case, a quasi-stationary excess carrier concentration distribution  $\Delta n(x,t)$  arises across the  $10 \mu\text{m}$  epilayer thickness after a relatively short transient stage of the initial carrier decay  $t \approx \tau_{\text{epi}}$  [3, 9]. The quasi-stationary distribution comprises to a constant of surface recombination fundamental mode which mathematically is described [10, 12]:

$$\frac{1}{\tau_S} = \alpha_0^2 D, \quad (7)$$

where  $\alpha_0$  is the smallest eigenvalue solution of the following equation:

$$\tan(\alpha_0 d) = (S_1 + S_2) \left( \alpha_0 D - \frac{S_1 S_2}{\alpha_0 D} \right). \quad (8)$$

The effective lifetime of the fundamental mode is then given by:

$$\frac{1}{\tau_{\text{eff}}} = \frac{1}{\tau_{\text{bulk}}} + \frac{1}{\tau_S}, \quad (9)$$

which is composed of two components. The first one arises from recombination in the volume of the semiconductor (bulk constant lifetime  $\tau_{\text{bulk}}$ ), the other component takes into account the contribution of recombination at the surfaces and generally is a function of surface recombination velocities and carrier diffusion coefficient.

To obtain value of  $\tau_S$  for given  $\tau_{\text{bulk}}$ ,  $d$ ,  $D$ ,  $S_1$  and  $S_2$  Eqs. (2–6) must be solved numerically for every single case. However, numerical calculation is not convenient if parameters are not known precisely, or if they obey slight variation with injection level and needs to be varied. Alternatively, an approximate analytical solutions for two limiting cases were established in Refs. [11, 12]. For  $S_1 = S_2 = S$  the fundamental mode carrier depth distribution in the sample is of the symmetrical form, which is illustrated in Fig. 3, a, (numerical calculations presented in Ref. [12]). In this case carrier diffusion flow is directed equally towards opposite directions and the appropriate solution for lifetime is given by [11, 12]:

$$\tau_S \cong \tau_{S_{app}} = \frac{d}{4S_1} + \frac{d}{4S_2} + \frac{d^2}{D\pi^2} = \frac{d}{2S} + \frac{d^2}{D\pi^2}. \quad (10)$$

The right hand side of this formula is composed of two terms which give the exact analytical surface lifetime solutions for  $Sd/D \gg 1$  and  $Sd/D \ll 1$ . The first term ( $d/2S$ ) can be interpreted as an effective time for recombination events at the surfaces if the diffusion component is fast enough [6]. The second term ( $d^2/D\pi^2$ ) can be interpreted physically as the time duration for excess carriers needed to travel the distance from the middle of the slab to the surface plane. In Ref. [11, 12] it was shown that the maximum error of Eq. (10) compared to a numerical solution is only 4%–5%, which arises at the intermediate ratio of parameters  $Sd/D \cong 1$ .

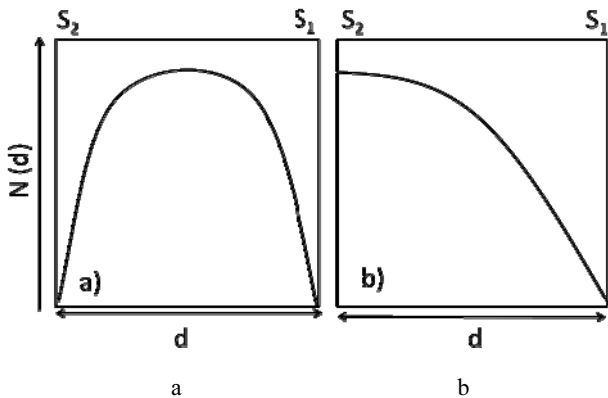


**Fig. 3.** Excess carrier quasi-stationary distribution across thin slab thickness for the homogeneous surface recombination case then  $S_1 = S_2$  (a) and the asymmetrical surface recombination case  $S_1 \gg S_2$  (b)

Another approximation for limiting conditions is when  $S_2$  (equivalently as  $S_1$ ) mathematically is set to zero. In the following we will assume that  $S_1$  (at the epi/substrate plane) is constant, determined by growth technique, and  $S_2$  (at the epi/film plane) can be varied, hence it can be much smaller than  $S_1$ . Therefore, when  $S_1 \gg S_2$  excess carriers recombine mainly at the epi/substrate surface with a higher SRV value  $S_1$ . This causes excess carrier diffusion flow towards the right side because of the asymmetrical distribution across the sample thickness (Fig. 3, b). As a result the surface recombination lifetime becomes [10]:

$$\tau_S \cong \tau_{S_{app}} = \frac{d}{S_1} + \frac{4d^2}{D\pi^2} \quad (11)$$

with the similar physical meaning for two terms on the right hand side as described for Eq. (10). The main difference of Eq. (11) from Eq. (10) occurs because of doubling the effective slab thickness for the carrier diffusion term. Note, that an approximation of Eq. (11) also gives a small maximum 4% error for the ratio  $S_1 d/D \cong 1$  in respect to the exact numerical resultant values [11].

According to the two possible limiting conditions as described above, we see that a difference within factor of 4 should be changed in two limiting cases. We have developed a formula for the intermediate cases of a surface recombination ratio  $S_1/S_2 > 1$ :

$$\frac{1}{\tau_{epi}} = \frac{1}{\tau_{bulk}} + \left( \frac{d}{k^2 S_1} + \frac{d}{k^2 S_2} + \frac{4d^2}{k^2 D\pi^2} \right)^{-1}. \quad (12)$$

Here  $k$  is a dimensionless coefficient developed empirically which confirms both the symmetrical (Eq. 10) and the asymmetrical (Eq. 11) cases:

$$k = 1 + 10^3 / \left( 10^3 + \left( \frac{S_1}{S_2} \right)^2 \right). \quad (13)$$

From Eq. (13), it follows that  $k = 2$  when  $S_1 = S_2$  and Eq. (12) becomes Eq. (10). When  $S_1 \gg S_2$ ,  $k = 1$ , and Eq. (12) becomes Eq. (11). When  $S_2$  is somewhere in between, Eq. (12) gives a smooth transition towards the other boundary condition. The coefficients were chosen empirically to fulfill a  $k$  value in a sufficiently large range of the  $S_1/S_2$  ratio.

The proposed model of the problem for a transient solution between symmetric and asymmetric SRV on two surfaces is not unique. Several more sophisticated mathematical models recently have been applied for carrier lifetime evaluation in 4H-SiC epilayers [9, 15]. We should note that reasoning for particular model highly depends on the experimental technique, the thickness of samples respect to laser light penetration depth, the temperature ranging and, of course, the goal of the study. Authors typically apply mixed simplified model together with a numerical prove of a particular case [12]. Since we are interested in the simple tendency of the SRV velocity reduction on the passivation scheme rather than on the actual SRV values, our model looks applicable for FCA type measurement under small epi thickness ( $d \ll 1/\alpha$ ) and a constant medium/high injection condition ( $\Delta n = \Delta p \gg n_0, p_0$ ) when a constant  $D$  value can be used at room temperature.

## MODEL APPLICATION

The next step is to simulate curves according to Eq. (10) and Eq. (12) versus epilayer thickness and different values of recombination parameters. Nomograms were drawn keeping one parameter variable. The diffusion coefficient was chosen to be  $D = 3.5 \text{ cm}^2/\text{s}$ , which is a common value for 4H-SiC established at room temperature for carrier injection of about  $10^{17} \text{ cm}^{-3}$  [13]. Excess carrier bulk lifetime is not know precisely in the epilayers and can be varied in the range  $\tau_{\text{bulk}} = 0.3 \mu\text{s} - 4 \mu\text{s}$  covering a typical range for values observed in a number of thick epi-growth 4H-SiC layers by CVD. In this paper we simulate

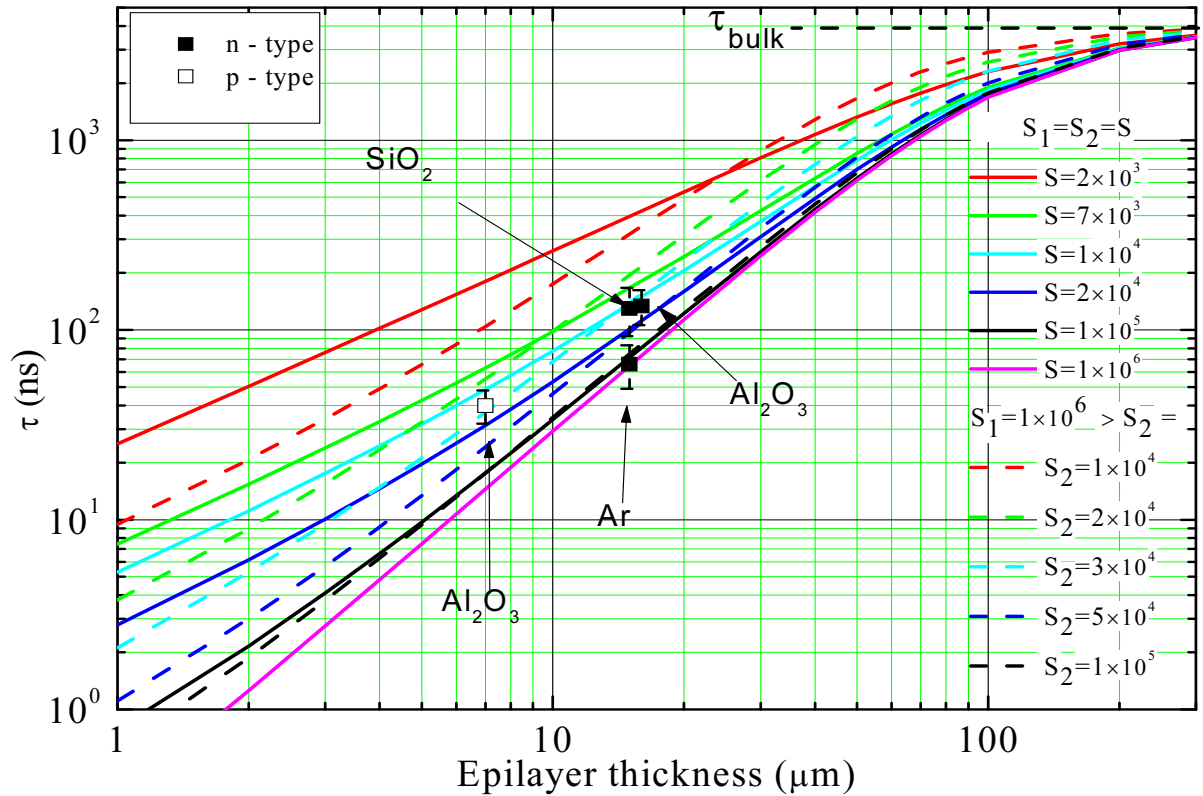


**Fig. 4.** Simulated nomograms for various SRV values are shown for effective carrier lifetime as a function of epilayer thickness. Points represent experimental results. Solid lines are constructed for the case  $S_1 = S_2$  Eq. (10) and dashed lines are constructed for the case  $S_1 > S_2$  Eq. (12) when  $S_1 = 1 \times 10^6$  cm/s. Other parameters in Eq. (10) and Eq. (12) remain constant  $\tau_{\text{bulk}} = 4 \mu\text{s}$ ,  $D = 3.5 \text{ cm}^2/\text{s}$

curves assuming the highest bulk lifetime, since the epilayer quality is improving annually [14]. The obtained experimental data from every sample is compared with two sets of nomograms in Fig. 4. The first set was made for the homogeneous case  $S_1 = S_2$  where various combinations of SRV were simulated from  $2 \times 10^3$  cm/s to  $1 \times 10^6$  cm/s as shown by solid lines. The obtained lifetimes (from Fig. 2) are also shown in respect to epilayer thickness. Lifetime values in n-type samples with  $\text{SiO}_2$  and  $\text{Al}_2\text{O}_3$  films and also p-type epilayer fit in between simulated lines of  $S_1 = S_2 = 1 \times 10^4 - 2 \times 10^4$  cm/s. Sample bombarded with Ar-ions indicated the highest SRV rates of  $10^5$  cm/s –  $10^6$  cm/s.

A second set of numerical nomograms was made for the asymmetrical carrier distribution case,  $S_1 > S_2$ , according to Eq. (12). Simulation was made assuming a high value of  $S_1 = 1 \times 10^6$  cm/s at the epi/substrate interface while  $S_2$  at epi/oxide interface varies depending on the top surface passivation. Simulated sets for  $S_2$  varying from  $1 \times 10^4$  cm/s to  $1 \times 10^5$  cm/s in Fig. 4 are shown in dashed lines. The fit gives a higher value of  $S_2$  for a passivated film surface ( $4 \times 10^4$  cm/s in n-type epilayer and about  $3 \times 10^4$  cm/s in p-type epilayer). The sample treated with Ar could be described again with SRV at  $S_2 > 1 \times 10^5$  cm/s, although Eq. (12) becomes Eq. (10) when  $S_2$  approaches  $S_1 = 1 \times 10^6$  cm/s.

The fit for the asymmetrical SRV case gives slightly higher  $S_2$  values than for the symmetrical case. To establish the actual SRV value it is crucial to know what is the

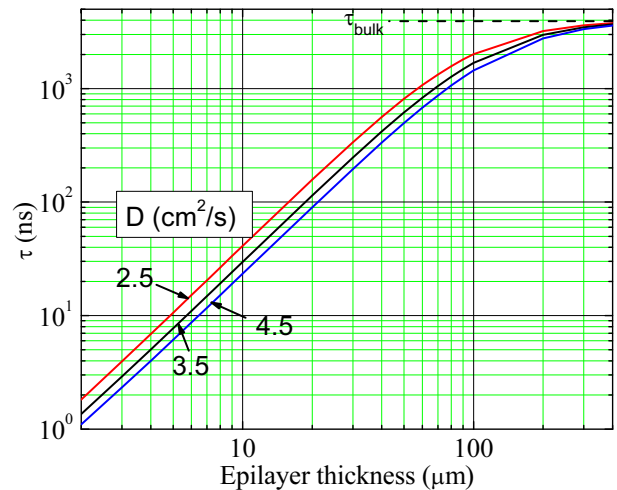


**Fig. 5** Influence of diffusion coefficient for SRV nomograms while other parameters remain constant  $\tau_{\text{bulk}} = 4 \mu\text{s}$ ,  $S_1 = S_2 = 5 \times 10^5$  cm/s. With increasing  $D$  same SRV curve shifts down describing lower carrier lifetime for the same epilayer thickness

value of the bulk lifetime. Also other parameters in Eqs. (10) and (12) can influence the evaluation of SRV value, for example, the sample treated with argon implantation can be explained by similar SRV of the order  $< 10^5$  cm/s if the  $\tau_{\text{bulk}}$  value is decreased down to  $\tau_{\text{bulk}} \cong 0.4 \mu\text{s}$ . So, the obtained SRV values correspond to the upper limits of practical case for lower  $\tau_{\text{bulk}}$ . Moreover,

the diffusion coefficient variation versus injection gives slight shift for nomograms. Since it depends on induced carrier concentration the excitation condition must be controlled precisely. In Fig. 5 the influence of the diffusion coefficient variation is evaluated. With increasing diffusion coefficient, curves describing the same SVR shifts downwards describing an area with lower carrier lifetimes.

Nevertheless small errors can occur if the mean experimental lifetime of  $\tau_{\text{epi}}$  is not defined properly from the experiment.

## CONCLUSION

We have presented a simple model for graphical evaluation of surface recombination velocity in 4H-SiC epilayers. Effective carrier lifetime was measured in the epilayers with the known thicknesses and incorporated between simulated SRV curves. We have found that the highest SRV was in the n-type epilayer untreated or treated with argon which yield limiting values,  $S = (10^5 - 10^6)$  cm/s. The n-type samples treated with SiO<sub>2</sub> and Al<sub>2</sub>O<sub>3</sub> showed similar lifetimes and SRV values which was well described for the case  $S_1 = S_2$  within  $(1 \times 10^4 - 2 \times 10^4)$  cm/s and for  $S_1 > S_2$  within  $(2 \times 10^4 - 4 \times 10^4)$  cm/s. The p-type epilayer was grown thinner and fitted within SRV values of about  $1.5 \times 10^4$  cm/s and  $3 \times 10^4$  cm/s, correspondingly. Also it is evident that thinner epilayer would shift SRV towards lower values for both presented models. In this case, a well defined statistical distribution of the experimental lifetimes in the epilayer prior and after surface passivation is much required in order to find the proper tendency in  $S_2$  variation. Finally, these simulations can be performed for various parameters sets and could be a useful tool for a fast surface recombination evaluation and optimization of various passivation films.

## REFERENCES

1. Casady, J. B., Johnson, R. W. Status of Silicon Carbide (SiC) as a Wide-bandgap Semiconductor for High Temperature Applications *Solid State Electronics* 39 1996: pp. 1409–1422.
2. Galeckas, A., Linnros, J., Frischholz, M., Grivickas, V. Optical Characterization of Excess Carrier Lifetime and Surface Recombination in 4H/6H-SiC *Applied Physics Letters* 79 (3) 2001: pp. 365–367.
3. Galeckas, A., Grivickas, V., Linnros, J., Bleichner, H., Hallin, J. Free Carrier Absorption and Lifetime Mapping in 4H SiC *Journal of Applied Physics* 81 1997: pp. 3522–3525.
4. Galeckas, A., Grivickas, P., Grivickas, V., Bikbajavas, V., Linnros, J. Temperature Dependence of the Absorption Coefficient in 4H- and 6H-Silicon Carbide at 355 nm Laser Pumping Wavelength *Physica Status Solidi (a)* 191 (2) 2002: pp. 613–620.
5. Grivickas, V., Galeckas, A., Grivickas, P., Linnros, J. Determination of the Polarization Dependence of the Free-Carrier-Absorption in 4H-SiC at High-Level *Materials Science Forum* 338–243 2000: pp. 555–558.
6. Luke, K. L., Cheng, L. J. Analysis of the Interaction of a Laser Pulse with a Silicon Wafer: Determination of Bulk Lifetime and Surface Recombination Velocity *Journal of Applied Physics* 61 (6) 1987: pp. 2282–2293.
7. Galeckas, A., Linnros, J., Grivickas, V., Lindefelt, U., Hallin, C. Auger Recombination in 4H-SiC: Unusual Temperature Behavior *Applied Physics Letters* 71 (22) 1997: pp. 3269–3271.
8. Grivickas, P., Galeckas, A., Linnros, J., Syvajarvi, M., Yakimova, R., Grivickas, V., Tellefsen, J. A. Carrier Lifetime Investigation in 4H-SiC Grown by CVD and Sublimation Epitaxy *Materials Science in Semiconductor Processing* 4 (1–3) 2001: pp. 191–194.
9. Klein, P. B., Myers-Ward, R., Lew, K. K., VanMil, B. L., Eddy Jr., C. R., Gaskill, D. K., Shrivastava, A., Sudarshan, S. Recombination Processes Controlling the Carrier Lifetime in n<sup>-</sup>4H-SiC Epilayers With Low  $Z_{1/2}$  Concentrations *Journal of Applied Physics* 108 (3) 2010: pp. 033713(1-11).
10. Grivickas, V., Linnros, J., Galeckas, A. Depth- and Time-Resolved Free Carrier Absorption in 4H SiC Epilayers: A Study of Carrier Recombination and Transport Parameters *Materials Science Forum* 264–268 1998: pp. 529–532.
11. Sproul, A. B. Dimensionless Solution of the Equation Describing the Effect of Surface Recombination on Carrier Decay in Semiconductors *Journal of Applied Physics* 76 (5) 1994: pp. 2851–2854.
12. Grivickas, V., Noreika, D., Tellefsen, J. A. Surface and Auger Recombinations in Silicon Wafers of High Carrier Density *Soviet Physics Collection* 29 (5) 1989: pp. 591–597.
13. Grivickas, P., Linnros, J., Grivickas, V. Carrier Diffusion Characterization in Epitaxial 4H-SiC *Journal of Materials Research* 16 2001: pp. 524–528.
14. Miyazawa, T., Ito, M., Tsuchida, H. Evaluation of Long Carrier Lifetimes in Very Thick 4H-SiC Epilayers *ECSCRM 8<sup>th</sup> Conference Proceedings, Oslo*, 2010.
15. Scajev, P., Gudelis, V., Jarasiunas, K., Klein, P. B. Fast and Slow Carrier Recombination Transients in Highly Excited 4H- and 3C-SiC Crystals at Room Temperature *Journal of Applied Physics* 108 2010: pp. 023705(1–9).

Presented at the National Conference "Materials Engineering'2010" (Kaunas, Lithuania, November 19, 2010)